Electronic Supplementary Material (ESI) for Green Chemistry.

Supporting Information

Controllable Exfoliation of Natural Silk Fibers into Nanofibrils by Protein Denaturant Deep Eutectic Solvent: Nanofibrous Strategy for Multifunctional Membranes

Xingxing Tan, Wancheng Zhao and Tiancheng Mu*

Department of Chemistry, Renmin University of China, Beijing 100872, China.

*Corresponding author. Tel: 86-10-62514925, E-mail: tcmu@ruc.edu.cn

Table of the contents

1. Methods and Discussions

The heating time and temperature are two important factors for successful exfoliation of silk fibers. When the heating temperature dropped to 80 °C, some of silk fibers were partially disintegrated while a few of silk fibers were still intact after 20 h (Figure S1), and more silk fibers could be disintegrated by increasing the heating time. After 4 days, the silk fibers/PD-DES mixture formed a gel-like material and the silk fibers were almost totally disintegrated into SNFs. When the heating temperature was increased to 100 and 120 °C, the optimal heating time to harvest SNFs/PD-DES gel-like material was 15 h and 7 h, respectively. In particular, most of the silk fibers were processed into rod-like fibers with diameters of 0.4 to 1 µm (Figure 1g) when the heating temperature was higher than 130 °C. These results shows that the exfoliation ability of PD-DES urea/GuHCl for silk fibers increases with increasing heating time and temperature, and the morphology of the product can be controlled by the heating temperature. In consideration of energy consumption, exfoliation efficiency as well as avoiding the destruction of silk by high temperature in exfoliation process, and also to simplify the experiment, the exfoliation condition to obtain SNFs was set as 90 °C for 20 h.

Porosity: The separator was immersed in distilled water for 6 h, and the porosity was calculated using the following equation (S1)[1]:

$$P\ (\%) = \frac{{M_b}/{\rho_b}}{{M_p}/{\rho_p} + {M_b}/{\rho_b}} \times 100\% \qquad (S1)$$

where P is the porosity of the SNF membranes (%), M_p is the mass of the SNF membranes (g), M_b is the mass of absorbed water (g), ρ_p is the density of the SNF membranes (g cm^{-3}), and ρ_b is the density of distilled water (1.0 g cm^{-3}).

Electrolyte uptake: The liquid electrolyte uptake was determined by immersing the separator into 1 M Na_2SO_4 aqueous solution at room temperature for 48 h and calculating using equation:

$$Uptake\ (\%) = \frac{W_1 - W_0}{W_0} \times 100\% \qquad (S2)$$

where W_0 and W_1 are the weights of the separator before and after immersion in the liquid electrolyte, respectively.

Ionic conductivity: The ionic conductivity was calculated using the following equation (S3):

$$\sigma = \frac{L}{R_b \times A} \qquad (S3)$$

where σ (S cm^{-1}) is the ionic conductivity, L (cm) represants the distance between the two electrodes, R_b (Ω) is the bulk resistance, A (cm^2) is the area of the stainless steel electrode.

Electrochemical Measurements

The specific capacitance (C, F g^{-1}), power density (P, W kg^{-1}) and energy density (E, Wh kg^{-1}) were valued from CP measurements using Equations S4–S6[2]:

$$C = \frac{4 \times I \times \Delta t}{m \times \Delta V} \qquad (S4)$$

$$E = \frac{C \times \Delta V^2}{4 \times 2} \qquad (S5)$$

$$P = \frac{E}{\Delta t} \qquad (S6)$$

where I (A) is the discharge current, m (g) is the total mass of active materials in the two electrodes, ΔV (V) is the voltage window excluding the voltage drop on the discharge process, and Δt (s) is the discharge time.

2. Supplementary Figures

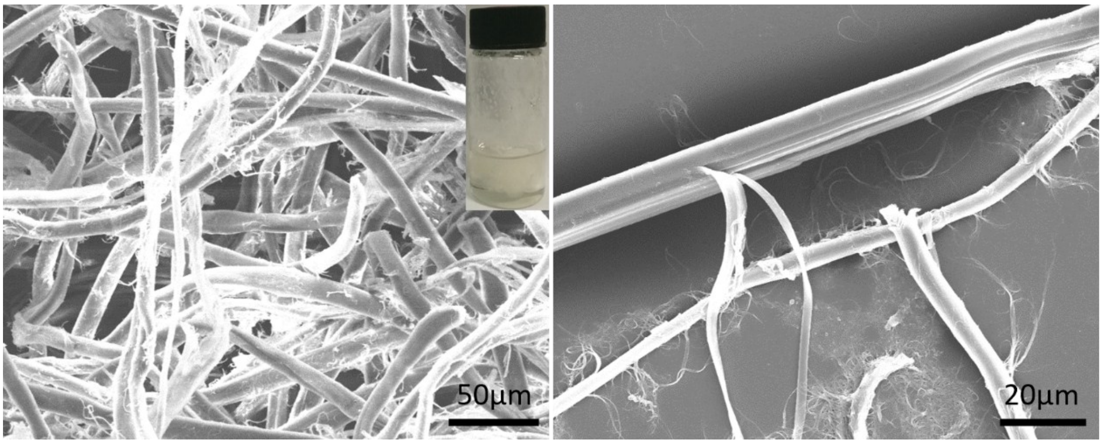

Fig. S1. Silk fibers/PD-DES mixture heated at 80°C for 20 h. The images show that some of silk fibers were partially disintegrated while a few of the silk fibers are still intact.

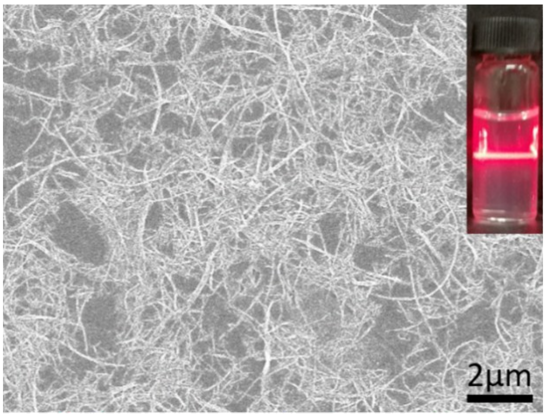

Fig. S2. SEM image of SNFs and photograph of aqueous dispersion (inset) obtained by centrifugation for 30 mins at 5000 rpm.

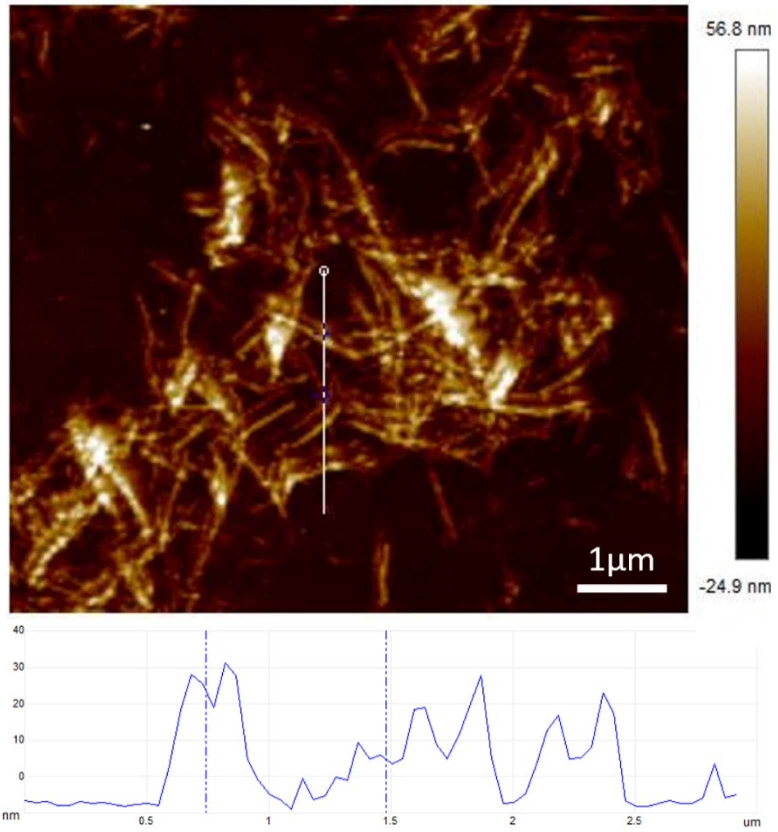

Fig. S3. Atomic force microscopy (AFM) image of SNFs obtained by centrifugation for 30 mins at 10000 rpm.

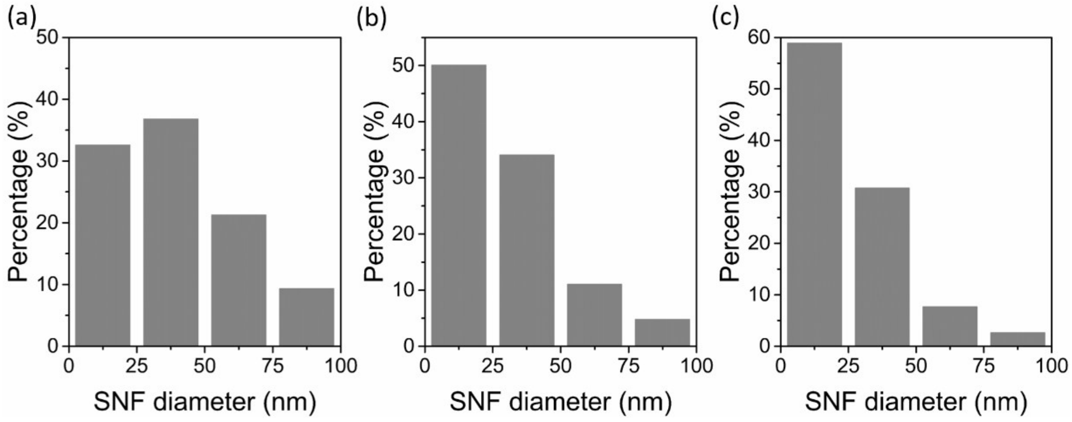

Fig. S4. Diameter distributions of SNF obtained by centrifugation speed of (a) 2000 rpm, (b) 5000 rpm, (c) 10000 rpm.

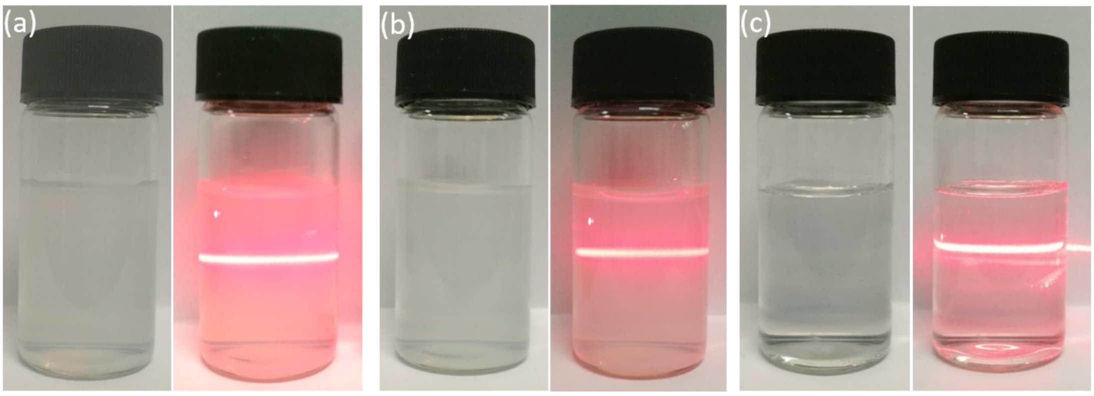

Fig. S5. Photographs of the aqueous suspensions of exfoliated SNFs, (a) fresh prepared, (b) stored for two weeks. The figures showed no obvious precipitation or aggregation in two weeks later. (c) turned to transparent when diluted to 0.04 mg mL^{-1}.

We measured zeta potential of SNF dispersions using Malvern Zetasizer Nano ZS90. Zeta potential data of SNF dispersions of fresh prepared and stored for two weeks obtained from the average of 3 results are -30.7 mV and -28.7 mV, respectively.

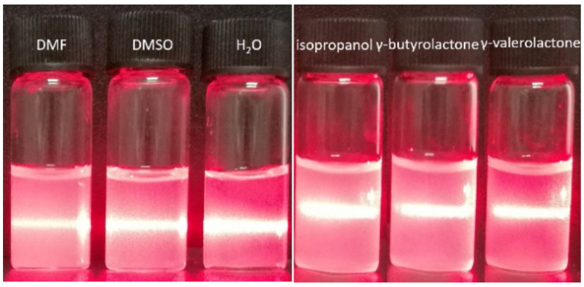

Fig. S6. Photographs of the aqueous suspensions of SNFs in different solvents.

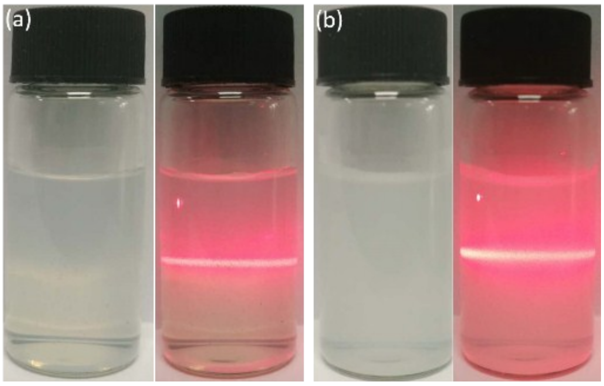

Fig. S7. Photographs of the aqueous suspensions of SNFs obtained by (a) stirring and (b) sonicating.

Fig. S8. Photograph of the scale-up SNF aqueous suspensions.

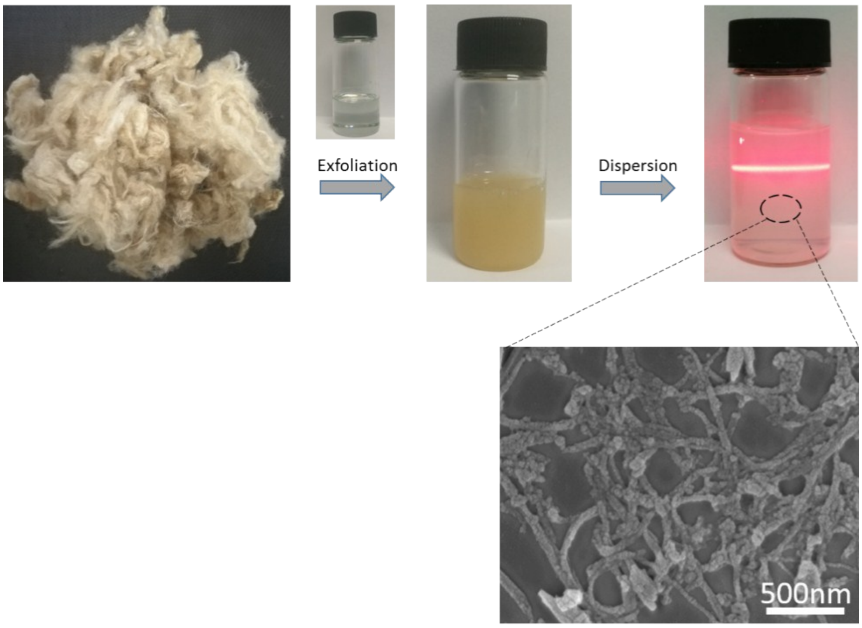

Fig. S9. Liquid exfoliation of tussah silk fibers by PD-DES urea/GuHCl.

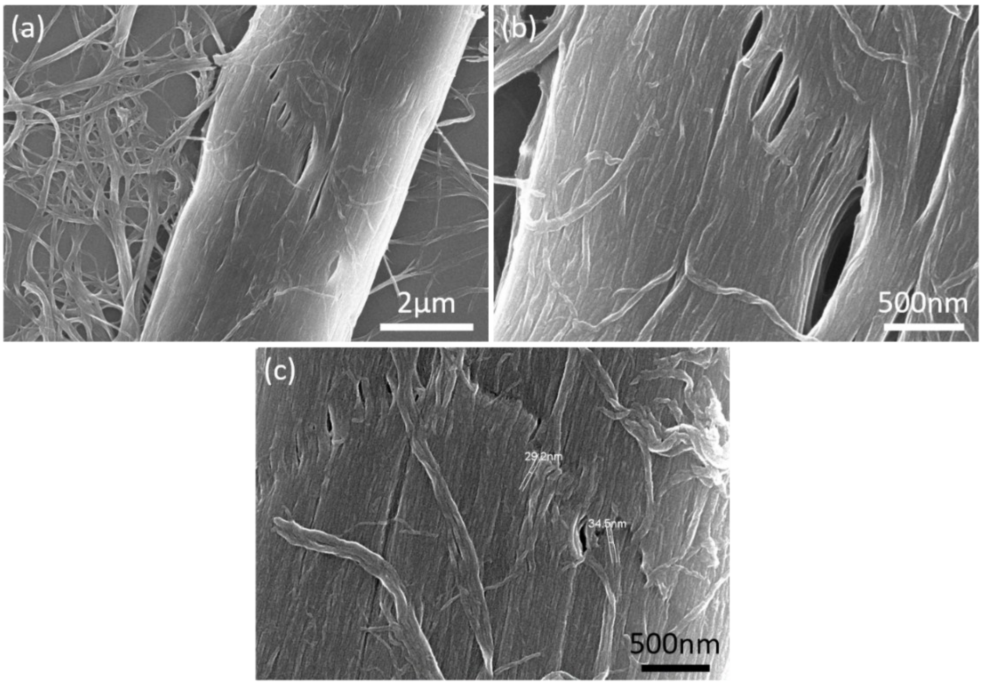

Fig. S10. SEM images of silk fibers disassemble into SNFs after PD-DES treating showing varied nanofibrillar structure.

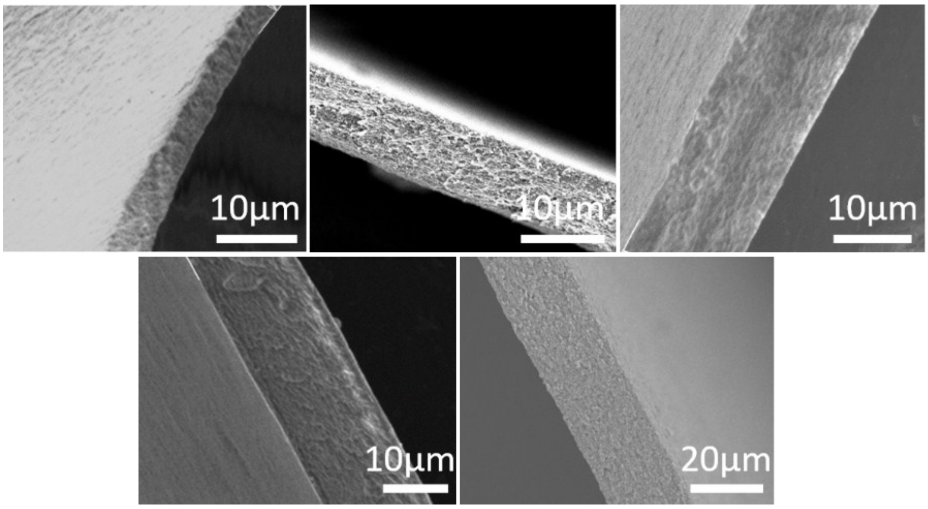

Fig. S11. The SNF membranes with different thickness.

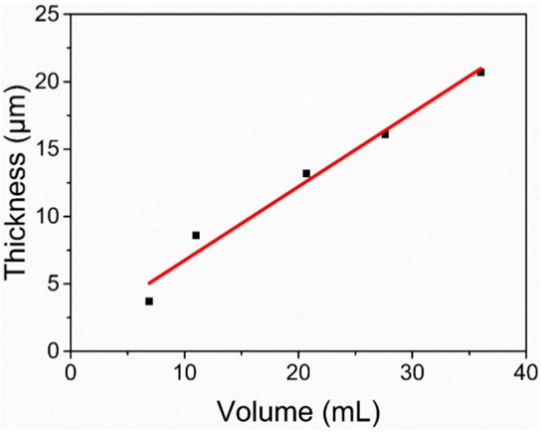

Fig. S12. The SNF membrane thickness versus the filtration volume of the SNF aqueous suspension (1.0 mg mL^{-1})

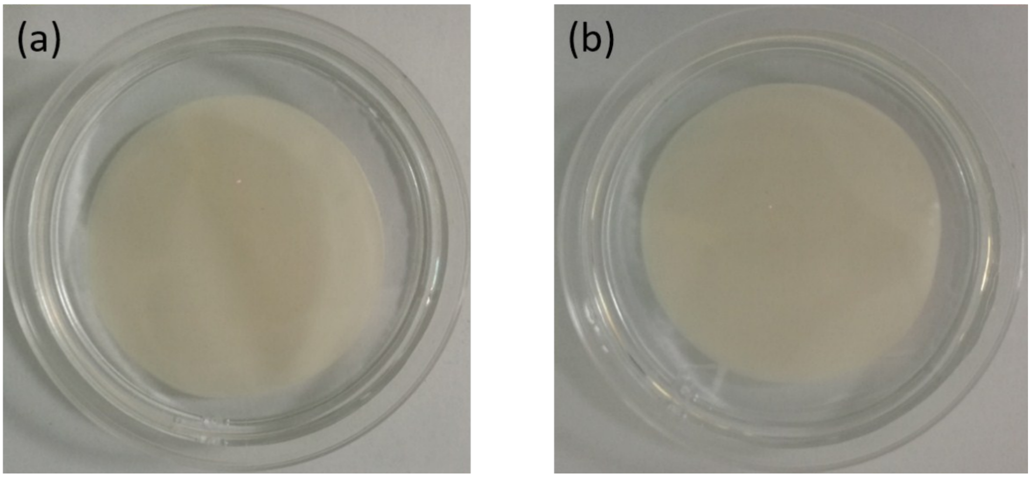

Fig. S13. Photographs of SNF membranes immersed in deionized water for (a) 10 mins, (b) five months. The figures showed the SNF membrane did not undergo dissolution in five months later.

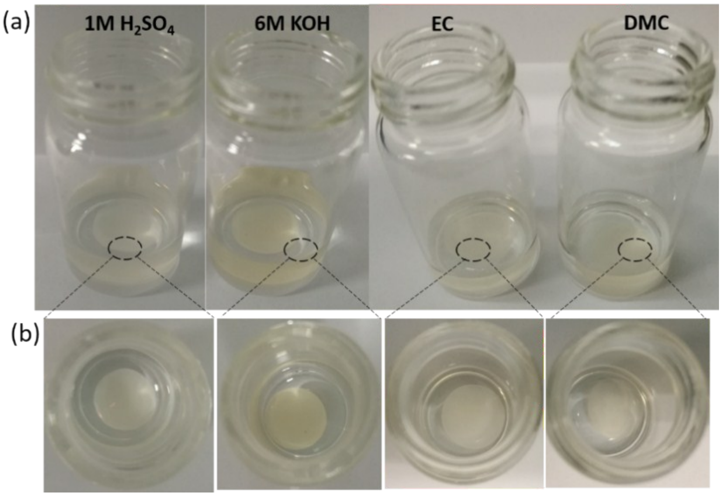

Fig. S14. Photographs of SNF membranes immersed in different systems for (a) 10 mins, (b) two weeks. The figures showed the SNF membranes did not undergo dissolution in two weeks later.

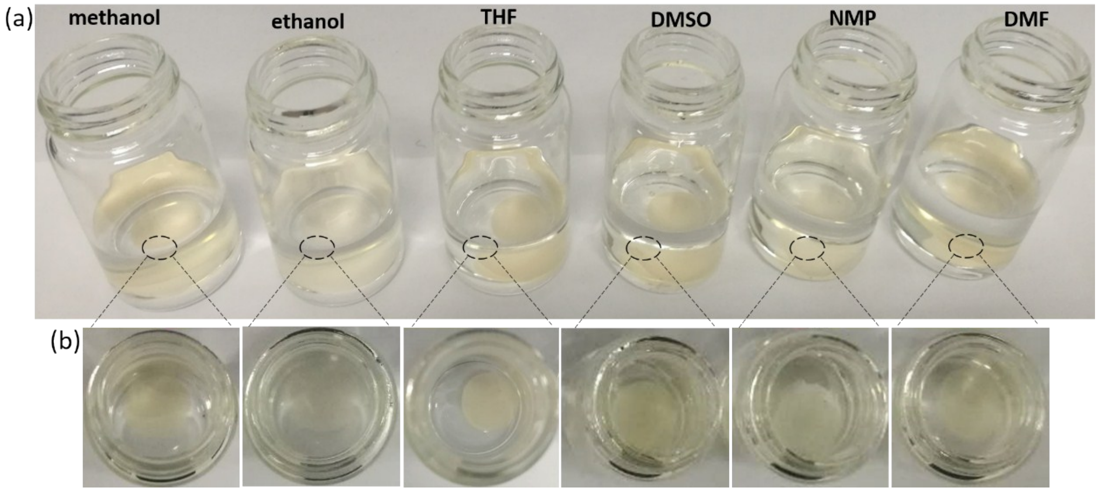

Fig. S15. Photographs of the SNF membranes immersed in different organic solvents for (a) 10 mins, (b) two weeks. The figures showed the SNF membranes did not undergo dissolution in two weeks later.

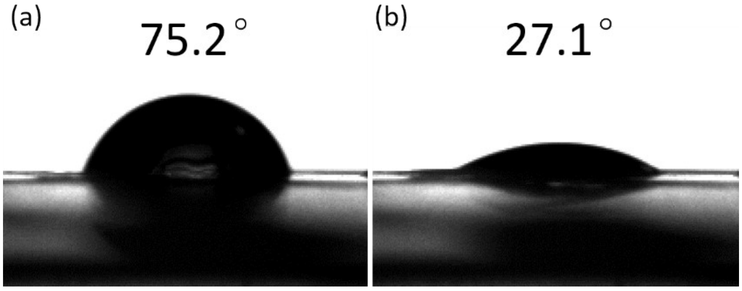

Fig. S16. Contact angle photos of a drop 1 M Na_2SO_4 solution on the SNF membranes in (a) 0 min and (b) 8 mins.

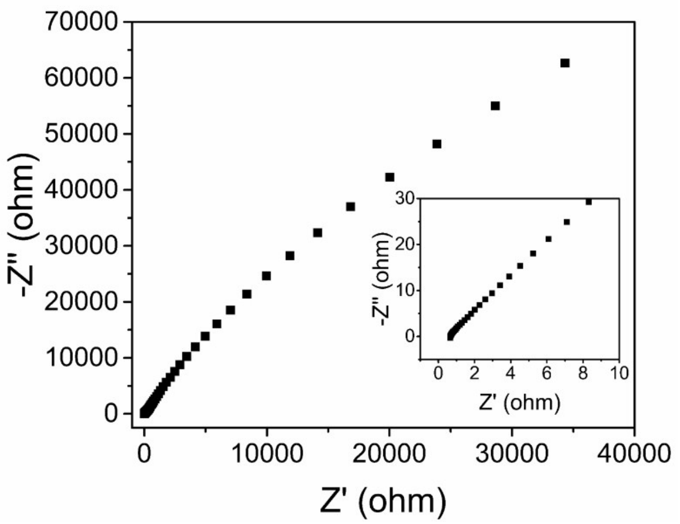

Fig. S17. Nyquist plots of the SNF separator.

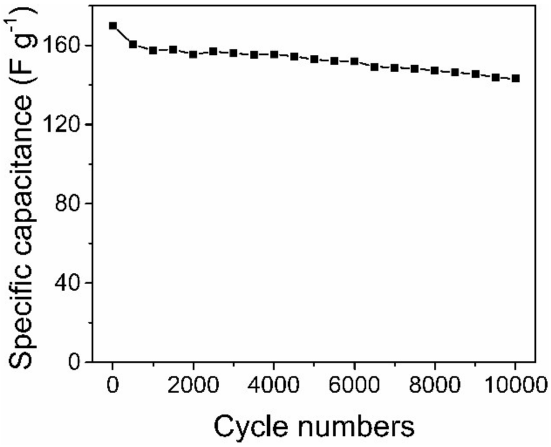

Fig. S18. Cycling performance measured at a current density of 1 A g^{-1}.

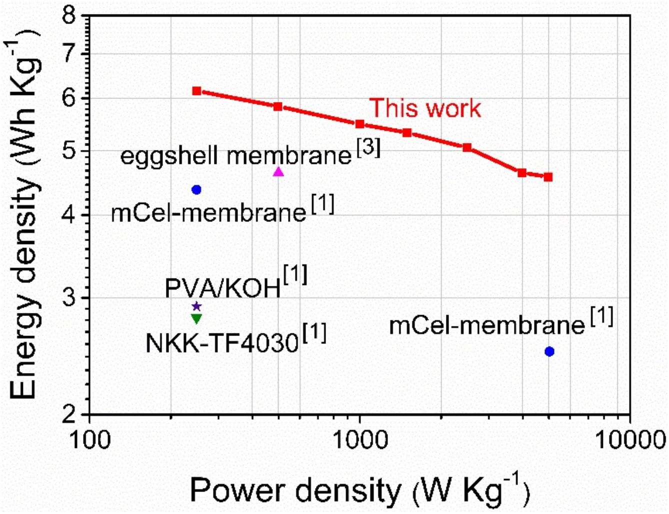

Fig. S19. Ragone plot for the SNF-membrane-based supercapacitor and a comparison with the previous reported separators (mCel-membrane,[1] PVA/KOH,[1] NKK-TF4030,[1] eggshell membrane[3]).

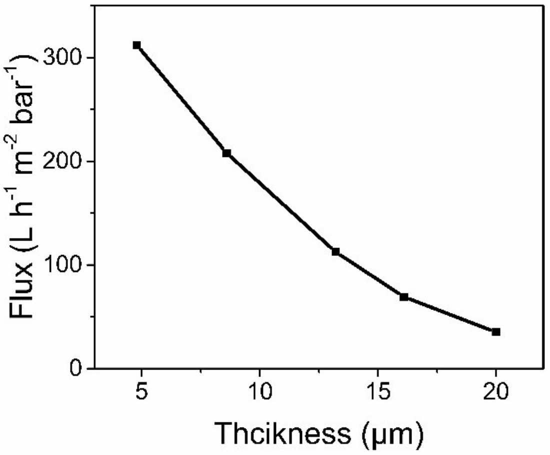

Fig. S20. Water flux of SNF membranes with different thickness.

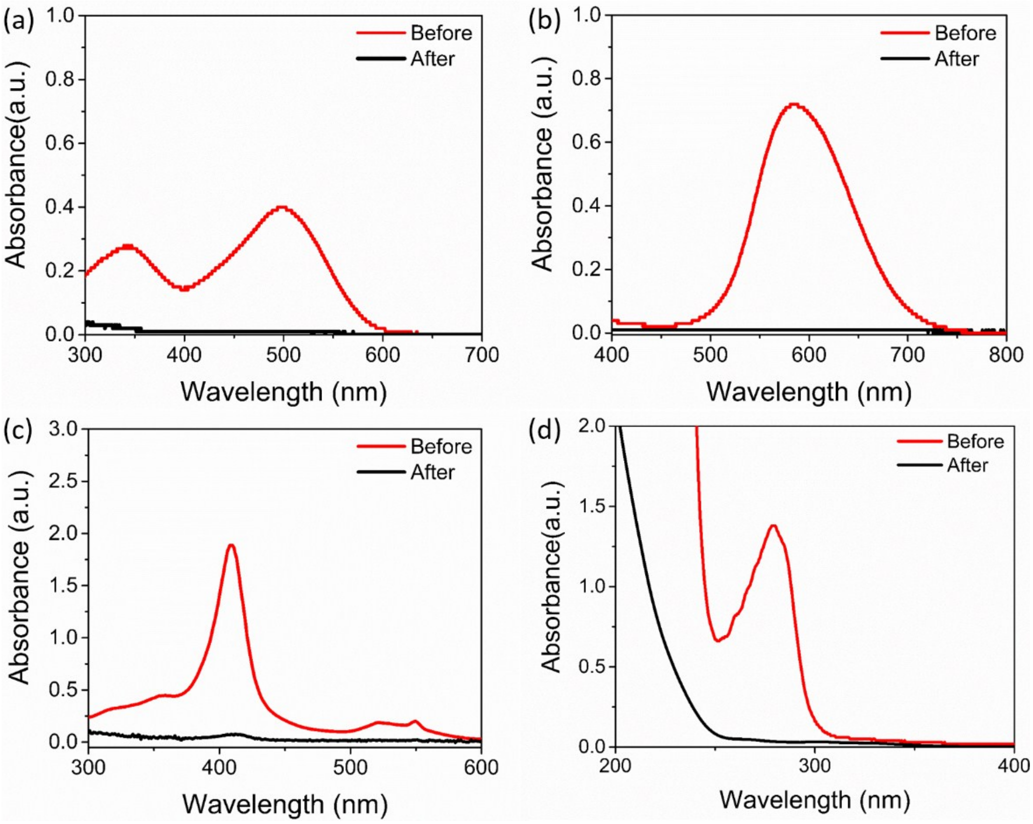

Fig. S21. UV-vis spectrum of (a) Congo Red, (b) Brilliant Blue G, (c) Cyt.c and (d) BSA aqueous solution before and after filtrated with SNF membranes.

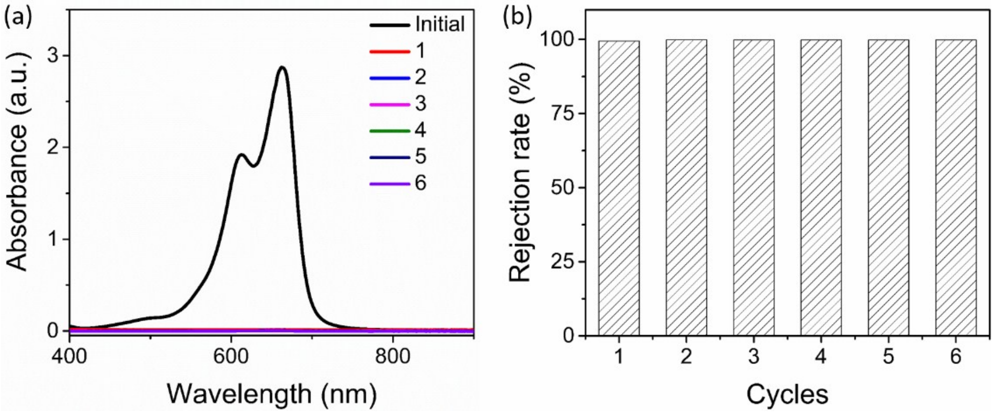

Fig. S22. (a) UV-vis spectrum of methylene blue aqueous solution before and after filtration. (b) Recyclability of SNF membrane after filtration. The membranes after each filtration were recycled by immersing in water or ethanol.

3. Supplementary Tables

Table S1. The lowest freezing point of urea/guanidine hydrochloride in different molar ratios.

mol urea (%)	**T_f (°C)**
33	118.6
50	93.2
67	60.3
75	80.6

Table S2. The effect of centrifugation rates on the concentration and yield of SNFs in the Liquid exfoliation of silk fibers by DES urea/guanidine hydrochloride.

Centrifugation rates (rpm)	**concentration (mg mL^{-1})**	**Yield (%)**
2000	1.0	70
5000	0.3	20
10000	0.02	1.2

Table S3. Mechanic comparison of SNF membranes with other SF-based and SNF-based materials in the literature.

Sample	**Ultimate Stress (Mpa)**	**Young's Modulus（Gpa）**	**Thickness (μm)**	**Reference**
SNF	62.75	2.95	10	This work
SNF	40	3.5	200	4
SNFS/ANF	52.4	2.4	～18	5
SF	67.7	1.9	200	6
SF/Silk Microfiber	40.1	0.325	—	7
SF/Cellulose	50-120	1.6-1.8	150	8
SF/Chitin Nanofiber	64-113	2.2-2.8	—	9
SF/Chitosan	32.8-119.7	1.07-5.73	—	10
SF/keratin	0.299	38.1	40	11
SF/Glycerol	20.39	1.38	—	12
SF fibrils/amyloid fibrils	3.9-7.8	1.08-2.25	200	13
regenerated SNF	～13	～1	200	13

4. Supplementary References

1. D. Zhao, C. Chen, Q. Zhang, W. Chen, S. Liu, Q. Wang, Y. Liu, J. Li and H. Yu, *Adv. Energy Mater., 2017, 1700739*.
2. L. Liu, B. Shen, D. Jiang, R. Guo, L. Kong and X. Yan, *Adv. Energy Mater.*, 2016, **6**, 1600763.
3. H. Yu, Q. Tang, J. Wu, Y. Lin, L. Fan, M. Huang, J. Lin, Y. Li and F. Yu, *J. Power Sources*, 2012, **206**, 463-468.
4. S. Ling, C. Li, K. Jin, D. L. Kaplan and M. J. Buehler, *Adv. Mater.*, 2016, **28**, 7783-7790.
5. L. Lv, X. Han, L. Zong, M. Li, J. You, X. Wu and C. Li, *ACS Nano*, 2017, **11**, 8178-8184.
6. H. J. Jin, J. Park, V. Karageorgiou, U. J. Kim, R. Valluzzi, P. Cebe and D. L. Kaplan, *Adv. Funct. Mater.*, 2005, **15**, 1241-1247.
7. G. Li, F. Li, Z. Zheng, T. Luo, J. Liu, J. Wu, X. Wang and D. L. Kaplan, *J. Mater. Sci.*, 2015, **51**, 3025-3035.
8. L. Zhou, Q. Wang, J. Wen, X. Chen and Z. Shao, *Polymer*, 2013, **54**, 5035-5042.
9. J. Jin, P. Hassanzadeh, G. Perotto, W. Sun, M. A. Brenckle, D. Kaplan, F. G. Omenetto and M. Rolandi, *Adv. Mater.*, 2013, **25**, 4482-4487.
10. J. G. Fernandez and D. E. Ingber, *Adv. Mater.*, 2012, **24**, 480-484.
11. H. Tu, R. Yu, Z. Lin, L. Zhang, N. Lin, W. D. Yu and X. Y. Liu, *Adv. Funct. Mater.*, 2016, **26**, 9032-9043.
12. S. Lu, X. Wang, Q. Lu, X. Zhang, J. A. Kluge, N. Uppal, F. Omenetto and D. L. Kaplan, *Biomacromolecules*, 2009, **11**, 143–150.
13. S. Ling, C. Li, J. Adamcik, Z. Shao, X. Chen and R. Mezzenga, *Adv. Mater.*, 2014, **26**, 4569-4574.